Smart Energy 21 (2026) 100218

Contents lists available at ScienceDirect

Smart Energy

journal homepage: www.journals.elsevier.com/smart-energy

A methodological framework for identifying District Heating Networks in Germany by utilizing the census data

Kai Droste *, Luca Döring, Jonas Klingebiel, Rahul Karuvingal, Dirk Müller

Institute for Energy Efficient Buildings and Indoor Climate, Mathieustraße 10, Aachen, 52074, North Rhine-Westphalia, Germany

ARTICLE INFO

Dataset link: https://github.com/RWTH-EBC/AixDHN

Keywords:
Urban planning
Census data
District heating
Shallow geothermal energy
Potential analysis

ABSTRACT

In this study, we present a methodological framework to identify the spatial position and heat demand of District Heating Networks (DHNs) for residential buildings in Germany by utilizing the census dataset for 2022. A clustering approach is used to locate DHNs and further datasets are included to derive and evaluate additional characteristics. A top-down calibration is applied to match the heat demand of the identified networks with validation data for 2022 from the Federal Statistical Office of Germany.

In total, 8,684 areas of presumed DHNs could be identified in Germany. 90 % of the demand is covered by about 10.87 % of the DHNs. The resulting dataset is published under the name District Heating Networks Dataset from Clustered Census Data (AixDHN)[1] on GitHub.

To demonstrate the application of the AixDHN dataset, a use case is presented in which the potential of Shallow Geothermal Collectors (SGCs) for supplying the identified district heating grids is evaluated. The use case reveals a technical potential of approximately 15.31 TWh/a for SGCs in Germany, supplying the heat for domestic buildings connected to the DHNs.

The AixDHN dataset provides a spatially detailed, transparent basis and enables the evaluation of the potential of further renewable heat sources for integration into DHNs. The methodology's strengths lie in its robust, generalized, and systematic approach, which makes it applicable throughout Germany without any further research on a regional level. It may act as a tool to support the planning and transformation of the heating sector towards renewable sources as well as municipal heat planning on a broad scope.

When cooling applications are addressed alongside heating, the economic viability of cold DHNs can be significantly improved, particularly enabling new applications in mixed-use areas that remain attractive even with lower heat densities.

1. Introduction

The EU has set the goal of achieving greenhouse gas neutrality by 2050 [1], and Germany aims to reach this goal by 2045 [2].

With about 50 % of the end-energy consumption, heating and cooling represent the largest energy consumption sector in Germany [3]. Currently, about 15.5 % of Germany's total heat demand is covered by DHNs [4], yet around 80 % of these networks still rely on fossil energy sources [5]. By 2030, the share of renewable sources for DHNs shall be increased to 30 %, which is part of the municipal heat planning concept in Germany [6,7]. Robust, spatially explicit data are essential to target interventions effectively, particularly as the role of DHNs is expected to expand in the coming years. Currently, there is a lack of comprehensive and reliable data on the status quo of DHNs in Germany. This study directly addresses this gap by developing the nationwide AixDHN dataset. Existing data sources include energy atlases from federal states [8], German Energy Efficiency Association for Heating, Cooling and CHP (AGFW) reports [9], the sEEnergies D5.1 District Heating dataset (sEE D5.1) database [10], the DEKADE-D-Waerme District Heating atlas [11], census data [12], and operator datasets [13]. Fleiter et al. [10] Wirtz et al. [14] However, these sources exhibit critical limitations that prevent their use as a comprehensive planning basis: Federal energy atlases vary significantly in temporal coverage (e.g., Baden–Württemberg relies on 2011 census data [8]) and spatial resolution, ranging from municipal aggregates to regional extracts. AGFW reports provide valuable aggregated statistics on heat generation and network

* Corresponding author.
E-mail address: kai.droste@rwth-aachen.de (K. Droste).

[1] https://github.com/RWTH-EBC/AixDHN.

https://doi.org/10.1016/j.segy.2025.100218
Received 7 August 2025; Received in revised form 7 November 2025; Accepted 28 November 2025
Available online 6 December 2025

characteristics, but lack any spatial information on network locations or extents. Fleiter et al. [10] combined 2018–2019 heat demand density datasets at hectare-level resolution (100 m × 100 m) to identify potential DHN areas, yet the approach relies on heat demand thresholds rather than actual connection data, introducing significant uncertainty. Pelda et al. [11] developed a district heating atlas with focus on network characteristics and supply structures, but coverage remains incomplete and spatial precision varies regionally. Wirtz et al. [14] examined exclusively 5th generation networks, representing only a small subset of Germany's DHN infrastructure. Energy atlases [8,11] Operator datasets [13] These limitations can be systematized into three fundamental gaps: (1) temporal inconsistency (datasets span 2011–2019 and miss recent expansion); (2) spatial coarseness (granularity ranges from municipal level to hectare-level aggregates, insufficient for building-level planning); (3) incomplete coverage (no single source provides a comprehensive nationwide identification of existing DHNs). Consequently, a spatially explicit, high-resolution, and temporally current dataset of German DHNs does not exist. This gap is critical for municipal heat planning (§ 26 WPG), which requires detailed spatial information to identify priority expansion areas, and for assessing the building-level feasibility of integrating renewable heat sources. Moreover, current transformation strategies lack a reliable baseline for evidence-based decision-making.

This study contributes: (1) A reproducible methodology to identify DHNs from 2022 census data at 100 m resolution. (2) AixDHN, the first nationwide, spatially explicit DHN dataset with demand estimates. (3) A demonstrated planning application via shallow geothermal collector potential assessment. Guiding questions: (1) How reliably can DHNs be detected from census-based heating unit distributions at 100 m resolution? (2) How can the resulting dataset inform the technical integration potential of renewable heat sources (exemplified by shallow geothermal collectors)?

To address the research question and provide a solid data basis for the transformation of the heating sector in Germany, Section 2 showcases a methodological framework to identify DHNs by utilizing the 2022 census data [15]. This dataset provides heating unit information for 100 m × 100 m grid cells across Germany, which is processed using a clustering algorithm to identify potential DHNs. Demand estimation is performed using hotmaps project data [16] and German statistical office datasets [17].

The developed framework is then applied to the 2022 census dataset and the resulting dataset's structure, the identified DHNs and key performance indicators of the networks are showcased and analysed in Section 3.

To demonstrate how this data can be applied to support planning activities in the heating sector, we present a use case in Section 4 where the dataset is utilized to estimate the potential of integrating SGCs in existing residential DHNs. For this purpose, the CLC dataset is applied to classify the surrounding areas of the DHNs into those suitable and those not suitable for SGCs.

The outcome of this study is further discussed in Section 5, where the results are also compared to other studies and datasets. Finally, Section 6 concludes the paper and discusses future work.

2. Methodology

This section is divided into two main parts. The first subsection outlines the methodological framework used to compile a dataset that captures the current state of DHNs supplying residential households across Germany. This dataset will be referred to as AixDHN. The second subsection details a straightforward approach, based on this dataset, to assess the potential of various renewable heat sources for integration into DHNs.

2.1. Identification and modelling of DHNs

The methodological framework aims to identify spatially explicit representations of DHNs in Germany and to derive their aggregated heat demand. The approach follows a data-driven, bottom-up design that links multiple geospatial datasets through analytical modelling and calibration steps. The method combines a geometric identification stage, which detects spatial clusters of residential district heating connections using density-based clustering, with an analytical attribution stage, which quantifies the corresponding heat demand through proportional scaling and top-down calibration. This combination ensures that both spatial and energetic dimensions of DHNs are represented within a consistent, reproducible framework.

The primary dataset used for DHN identification is the 2022 German Census, which provides heating system information for residential buildings on a 100 m grid [15,18]. Among central building heating systems, self-contained systems within apartments and other, less common types, heat supply through thermal grids, also known as District Heating (DH), is explicitly listed. Each grid cell i contains the number of apartments connected to DH ($h_{i,DH}$) and the total number of heated apartments ($h_{i,tot}$). This indication is bound to residential apartments, because the underlying survey did not address owners of commercial or industrial spaces. Thus, this study can only present insights into the state of DHNs supplying the residential sector. The dataset can be visualized in the online map application of the census 2022 [12]. As an example, Fig. 1(a) depicts the amount of apartments supplied by DH for the region of *Aachen*.

In the following, two pieces of information are extracted from every grid cell i for further analysis:

1. Is at least one apartment present, that is supplied by DH? ($\rightarrow h_{i,\mathrm{DH}} > 0$)
2. What is the portion of apartments that is supplied by DH in relation to all heated apartments? ($\rightarrow h_{i,\mathrm{DH}}/h_{i,\mathrm{tot}}$)

By reducing the positional data of each cell to its centroid, a point cloud is generated comprising all cells that satisfy the first condition. This point cloud can be interpreted as a spatial probability field, representing the likelihood of DH infrastructure presence. Considering the importance of high heat demand density for ensuring the economic and technical feasibility of DHNs [10,19], such networks can therefore be conceptualized as spatially contiguous regions characterized by elevated densities of connection points. Consequently, clustering algorithms that detect dense aggregations in spatial data are particularly suitable for DHN identification, provided that the spatial resolution of the underlying dataset is sufficiently fine to capture the distribution of residential heating systems.

To identify contiguous clusters of such points–representing presumed DHNs–a Density-Based Spatial Clustering of Applications with Noise (DBSCAN) algorithm is employed [20]. DBSCAN was selected because it does not require predefined cluster counts, can detect arbitrarily shaped clusters, and is robust to noise and outliers. Unlike centroid-based methods such as k-means, which assume convex cluster shapes and homogeneous point densities, DBSCAN identifies clusters purely from local point densities.

The algorithm depends on two parameters: ε (Euclidean neighbourhood radius) and $min_{samples}$ (minimum points to form a cluster). Their selection controls the spatial continuity of detected networks. The algorithm's basic method of operation is illustrated in Fig. A.8. To account for heterogeneity between dense urban and sparse rural areas, DBSCAN is applied in two passes with increasing ε values. Within the second pass we reuse all left-over, non-clustered points and attempt to cluster them again with an increased ε. This method attempts to achieve a compromise between a more defined cluster shape in dense urban areas and a looser connectivity between points in rural areas. The utilized parameters (1) were determined empirically by comparing

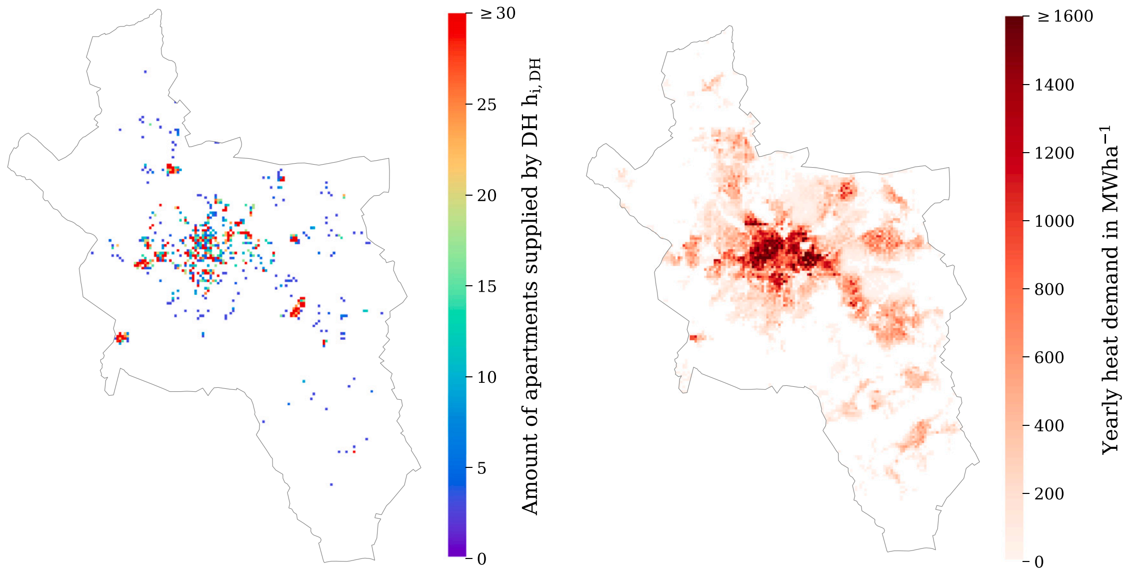

(a) Amount of apartments supplied by DH in *Aachen* based on the 2022 census (grid edge length: 100 m) [15].

(b) Yearly residential heat demand for Aachen according to hotmaps [16].

Fig. 1. Spatial distribution of district-heated aparatements and annual residential heat demand in the city of Aachen.

resulting cluster shapes to known DHN extents from municipal utility maps, as seen in Fig. 7(a). Although heuristic, this calibration ensures that the method produces realistic network morphologies within the constraints of census data granularity.

$$\epsilon_1 = 600m \qquad min_{\text{samples},1} = 3 \qquad \epsilon_2 = 1000m \qquad min_{\text{samples},2} = 3 \tag{1}$$

After determining a cluster, we draw a concave hull around the cluster's points utilizing an open-source algorithm [21] (concavity parameter: 1.4) to create a polygon and thus define a **presumable DHN** j that contains the grid cells C_j enclosed within the polygon A_j. From this, we can derive all geographical information that might be of interest for a use case, such as area, location and shape.

Furthermore, we aim to attribute a yearly heat demand to each found DHN. In order to achieve this, a heat demand map from the open-source EU project **hotmaps** [16,22] is used. The map features information on the residential yearly heat demand on a 100 m grid and is therefore well compatible with the census data. Firstly, we apply a top-down calibration to match more recent information on Germany's residential heat demand [23] by applying a uniform scale factor to the dataset. We further estimate that the specific heat demand of all apartments within each cell is similar and independent of their individual age and condition. We then employ a proportional allocation by assuming that the share of the residential heat demand Q_i within the cell i that is supplied by DH can be represented by $h_{i,\text{DH}}/h_{i,\text{tot}}$. The yearly heat demand Q_j of a presumed DHN j can then be calculated by summing the products of the portion of apartments supplied by DH and the residential heat demand Q_i for each cell $i \in C_j$:

$$Q_j = \sum_{i}^{C_j} \left(\frac{h_{i,\text{DH}}}{h_{i,\text{tot}}} \cdot Q_i \right) \tag{2}$$

The results are post processed by uniting DHNs that lie within another networks's area and removing small DHNs with a yearly heat demand below the threshold of 200 MWh/a. This limit is used to disregard unrealistically small DHNs and was established by estimating the demand of 10 to 15 single-family houses based on [24].

To further ensure the plausibility of the estimated DH demands, we apply a second top down calibration on state-level by comparing the sum of the demand of all DHNs within a state s to the delivered heat Q_s according to the states' offices for statistics from 2022 [17]. For the states *Bremen*, *Rheinland-Pfalz* and *Saarland* the data was not published to satisfy requirements of confidentiality. We derive a linear scaling factor β_s for each state s to adjust the DHNs' demands according to the validation data as shown in Eq. (3). A visualization of the calibration process is displayed in Appendix B.

$$Q_s \overset{!}{=} \sum_{j}^{j \in s} \beta_s \cdot Q_j \quad \forall\ s \tag{3}$$

Lastly, the share of the total residential heat demand within the DHN's area that is attributed to the DHN itself is calculated. For this, the DHN's estimated demand prior to the second calibration is used to avoid a distortion of the data, since just the demand related to DHN is scaled throughout that process.

2.2. Use cases for renewable energy potential analysis

By following the method for identifying DHNs in Germany and deducing viable information such as location and approximate annual heat demand, this data can be used to estimate the potential for integrating renewable heat sources into these networks.

In this study, we propose an algorithm for linking heat sources to DHNs with respect to spatial reachability and demand. For any type of heat source, the following inputs must be available:

- Geographical information on the availability of a heat source
- Methods of calculation for determining the expected extractable heat

The former may be delivered either as point data or as area data. Point data is suitable for instance in the cases of extraction points of deep geothermal energy or excess heat from industrial sites, whereas area data is preferred for technologies that scale primarily by occupied area, such as solar thermal energy or shallow geothermal energy.

We introduce two spatial parameters to evaluate if a heat source k is within reach of a presumable DHN j. The shortest possible connection between the DHN's area A_j and the point of heat integration of source k must not exceed the maximum distance $L_{connection}$. In the case of area sources the point of heat integration may be the area's edge point closest to A_j. This parameter symbolizes the length of a theoretical pipeline necessary to supply the extracted heat to the DHN. Secondly,

Table 1
Overview of AixDHN dataset attributes.

Attribute	Description	Unit	Type
ID	Unique identifier of DHN	–	*str*
GEN	Geographical name of administrative area	–	*str*
ARS	Regional key of administrative area	–	*str*
LAN	State (Bundesland)	–	*str*
geometry	Polygon of presumed DHN	EPSG:3035 Coordinates	*Polygon*
area	Area of presumed DHN	km^2	*float*
centroid	Centroid of presumed DHN	EPSG:3035 Coordinates	*Point (WKT)*
DH_demand	DH annual demand of private households	MWh/a	*float*
total_demand_cells	Total annual heat demand of private households in cells with DH demand	MWh/a	*float*
total_demand_area	Total annual heat demand in area of presumed DHN	MWh/a	*float*
share_DH	Share of DH demand in area of presumed DHN	%	*float*
heat_density_DH	DH_demand divided by area	$\mathrm{GWh/(a\,km^2)}$	*float*
heat_density	total_demand_area divided by area	$\mathrm{GWh/(a\,km^2)}$	*float*
DH_supplied _households	Households supplied by DHN	–	*int*
DH_cells	Cells that contain DH demand and form DHN area	EPSG:3035 Coordinates	*list of [int, int] (JSON serialized)*

we define a maximum distance surrounding the DHN L_{radius} that limits the usability of a heat source. This parameter is only applicable for area sources and equals $L_{connection}$ for point sources.

We then iterate over all DHNs in descending order of heat demand to prioritize the assignment of heat sources to DHNs with higher demand. Within each iteration, suitable heat sources are selected by applying the introduced parameters using a perimeter sweep.

The order of tested sources in every iteration is dependent on the order of the provided database of heat sources. Assuming that the order in which heat sources are listed within a database is not considered a crucial aspect of the input, the algorithm behaves non-deterministically, as an altered order of the input database yields a different output. If the available heat sources featured different priorities in terms of their usage, an initial sorting procedure within the database would be necessary.

Useable sources, that have not been linked to other DHNs in previous iterations, are assigned to the DHN until its demand is met or no more available sources are in range. In the case that during an iteration an available source provides more heat than can possibly be used in the supplied DHN, the assigned potential of said network is capped to the maximum usable heat and any leftover potential is neglected. The database is finally updated with the newly assigned sources to avoid double use in further iterations. The algorithm is depicted in Fig. A.9.

3. Results

3.1. Dataset structure

This study presents the novel AixDHN on DHNs in Germany. The dataset is distributed as *.geojson* file and its structure is illustrated in Table 1 and explained in the following section. Additionally, this dataset can be accessed on GitHub[2] [25].

[2] https://github.com/RWTH-EBC/AixDHN

Each DHN is identified by an **ID** and its location within Germany is specified by several administrative codes **GEN**, **ARS** and **LAN** according to the official nomenclature of administrative areas [26].

Its geographic location is defined by the **geometry** field, which is the primary geometry column and is read directly from the *.geojson* format. The according **centroid** is included and expressed in the Well Known Text (WKT) format [27]. Furthermore, all cells' coordinates that form the grid area are enclosed as JSON serialized string in **DH_cells**. Appropriate python snippets for reading in the AixDHN dataset are included in the repository. The DHN's calculated demand is given in **DH_demand** as well as the amount of apartments supplied in **DH_supplied_households**. The total residential heat demand, independent of the type of heating system, within the network's entire area is defined in **total_demand_area**, whereas **total_demand_cells** only describes the demand within cells that contain apartments supplied by DH. Furthermore, the demand share of DH in accordance to the explanation in Section 2 is presented the field **share_DH**. Lastly, the heat density of found DHNs is contained within the dataset. We distinguish between **heat_density_DH**, which is calculated utilizing the demand that is attributed towards the present grid and given in **DH_demand**, and **heat_density**, that takes the total residential heat demand in the found grid area (**total_demand_area**) into account.

Fig. 2 shows an exemplary map of *Aachen* with its identified DHNs and highlights the included attributes for one DHNs. Fig. B.10 depicts an overview of all found DHNs in Germany.

3.2. Analysis

The following section presents interim results that are of interest and analyses the final AixDHN dataset.

Throughout the methodology, 6,276,096 of 6,446,428 and therefore 97.36 % of apartments with an presumed connection to a DHN according to the census [18] have been clustered to form a total of **8,684 DHNs**. The utilized connection points are distributed among 279,447 cells of 100 m × 100 m. After converting the clusters of points to polygons, the

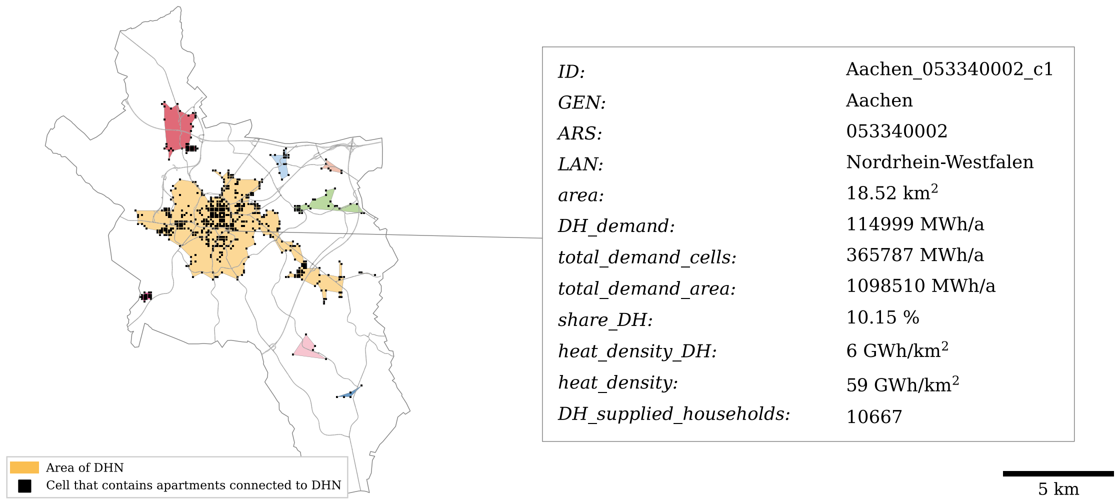

Fig. 2. Preview of results of the AixDHN dataset for region of *Aachen*.

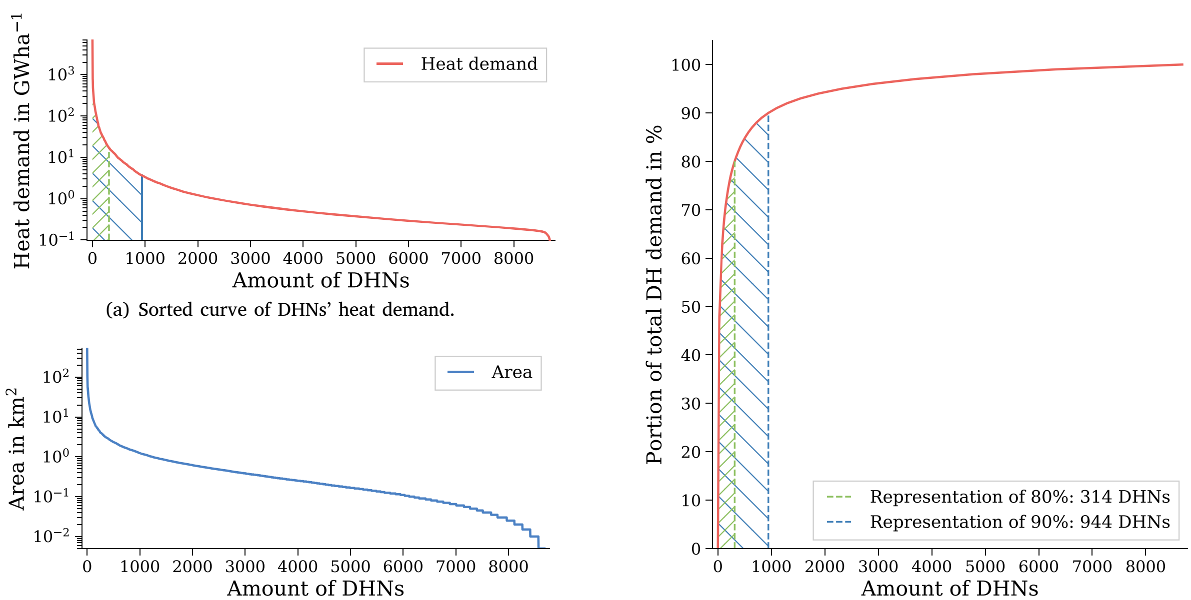

(a) Sorted curve of DHNs' heat demand.

(b) Sorted curve of DHNs' area.

(c) Amount of DHNs (sorted by descending heat demand) needed to represent a portion of the total heat demand of all DHNs (50.16 TWh).

Fig. 3. Sorted curves of German DHNs showing their heat demand, area, and the portion of the total national district heat demand they represent.

sum of all networks contain an area of 8,146.13 km^2 and represent a yearly heat demand of 50.16 TWh.

An analysis of the derived data shows that 72.09 % of networks contain an area smaller than 0.5 km^2. On the other hand, the biggest 1 % of networks in size represent approximately 41.21 % of the total network area. A similar observation can be made concerning the heat demand. The highest demand is featured in Berlin with a yearly demand of 7.05 TWh and therefore 11.55 % of Germany's total demand, followed by Hamburg with 3.66 TWh and Munich with 1.78 TWh, whereas a majority of 73.31 % of DHNs demand less than 1 GWh/a. Fig. 3(a) and Fig. 3(b) illustrate these observations through the sorted curves of area and heat demand for all found DHNs. To further emphasize the varieties in the networks' demands, Fig. 3(c) depicts the amount of largest DHNs in terms of demand that is necessary to represent a certain portion of the total DH demand. This diagram shows that for instance the 944 most demand-intensive DHNs are necessary to represent a share of 90 % of the total residential DH demand, as visualized by the blue hatched area.

Furthermore, Fig. 4(a) depicts the correlation between heat demand and occupied area of found networks on a logarithmic scale. To establish a visual reference to the previous figure, the scatter points are coloured according to the hatched areas in Fig. 3. For example, the green points visualize those DHNs necessary to represent a share of 80 % of the total residential DH demand. The samples' size in the scatter plot additionally indicates the heat density **heat_density_DH**. The histograms in Fig. 4(b) visualize the attributes **heat_density_DH** and **heat_density** as explained previously in this section. The attribute **heat_density** shows a mean of 42.3 GWh/(a km^2) and a standard deviation of 35.7 GWh/(a km^2), respectively **heat_density_DH** a mean of 5.6 GWh/(a km^2) and a standard deviation of 8.2 GWh/(a km^2). This figure is going to be addressed later in Section 5 for further discussion.

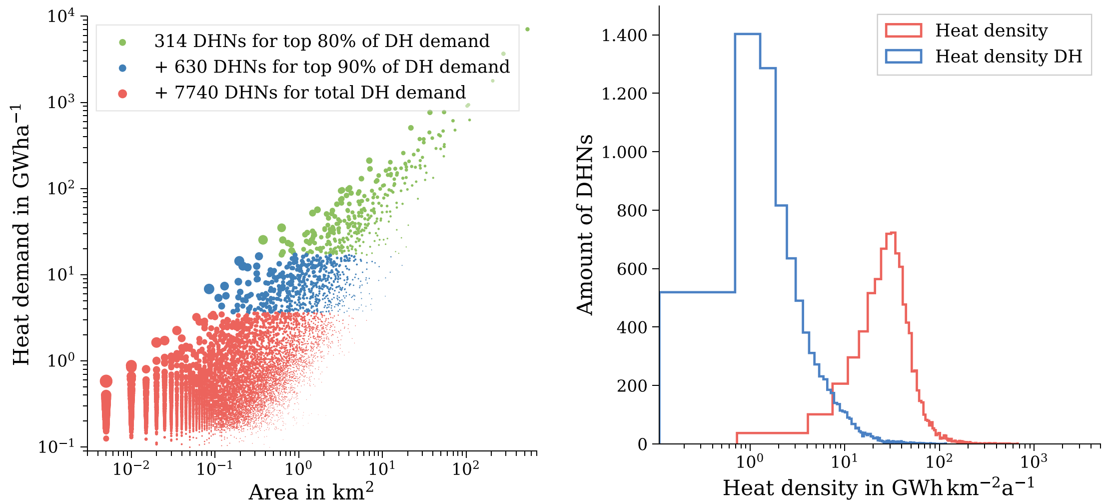

(a) Correlation between demand and area of DHNs. The sample size visualizes the heat density related to the DH demand (attribute **heat_density_DH**).

(b) Histogram of heat densities. Total heat demand respectively DH demand divided by DHN area (attributes **heat_density_DH** and **heat_density**).

Fig. 4. Overview of heat density characteristics for DHNs.

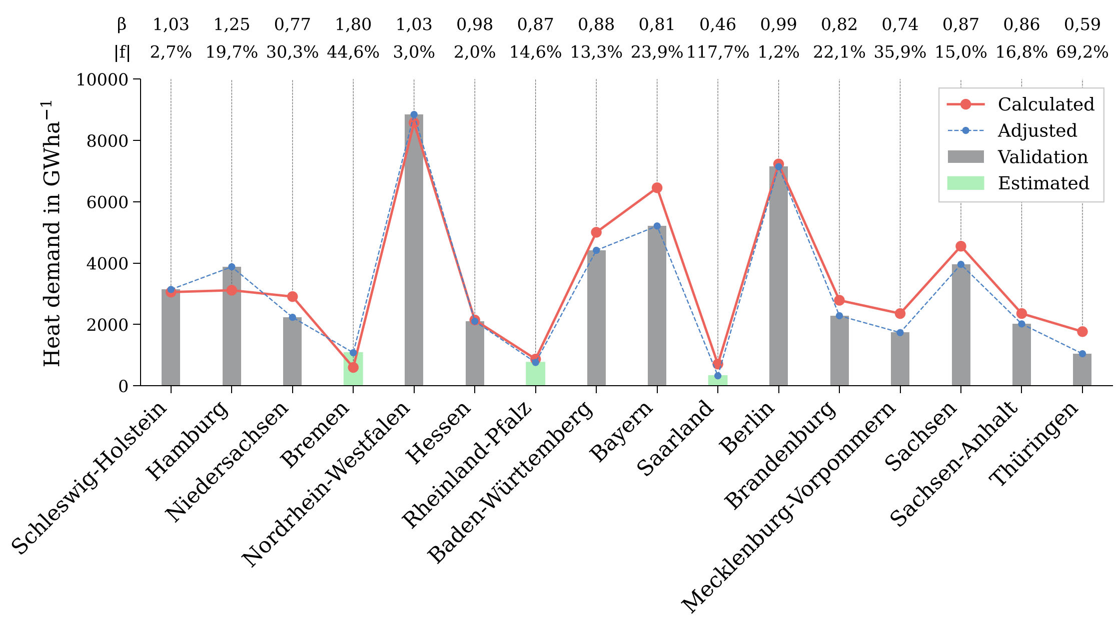

Fig. 5. Calibration of DHNs' heat demand per state. The red curve depicts the initial result according to Section 2.1, followed by the calibration (dotted blue line) to match the validation data (grey and green bars). The necessary scaling factor β and the relative error $|f|$ between calculated data and validation data is displayed above.

According to Eq. (3), the DH demand of all DHNs within each state is aggregated, compared and finally scaled according to data by the states' offices for statistics from 2022 [17]. The comparison of the initially calculated results and the validation data shows qualitatively well matching results, as depicted in Fig. 5. 4 states show relative deviations $|f|$ lower than 3 %, while a majority of 9 states feature moderate deviations from 13.3 % to 35.9 %. The highest deviations of 44.6 %, 69.2 % and 117.7 % are seen in 3 of the 4 states with the smallest DH demand. Absolute deviations range from 41.6 GWh/a to 1,245.8 GWh/a. The average absolute deviation corresponds to 469.4 GWh/a and the standard deviation is 318.2 GWh/a. In order to adjust the states' respective demands, scaling factors β_s from 0.46 to 1.80 are employed. The average scaling factor corresponds to 0.94 and the standard deviation to 0.31.

4. Use case

Following the general procedure described in Section 2.2, this section describes the specific use case of evaluating the potential of SGC for integration into DHNs in Germany.

4.1. Background on shallow geothermal collectors

SGC systems are horizontal heat exchangers installed near the surface, typically within the upper 5 m of the soil, but most commonly at depths of 1.2 m to 1.5 m below ground level [28,29]. SGCs consist of long polyethylene pipe networks that form a closed loop, in which a water-antifreeze mixture (brine) circulates. The brine serves as the transfer medium by adsorbing heat from the surrounding ground and delivering it to its consumer. Typical extraction temperatures range from 8 °C to 15 °C, with a temperature difference between flow and return of approximately 3 K to 4 K [30]. SGCs are typically used in combination with a heat pump to rise the temperature level to satisfy the requirements for space heating and domestic hot water supply. This application is typically denoted as Ground Source Heat Pump (GSHP). The utilization of Shallow Geothermal Energy (SGE) is possible everywhere from a geological perspective. Its potential is locally influenced by heat flux through solar radiation and precipitation [31]. Soil properties like density, porosity and water content, as well as climate conditions determine the extractable heat and must therefore be taken into account [32]. The primary challenge for planning and integration of SGCs is defining suitable and preferably undeveloped land upon which collector systems can be installed.

4.2. Potential analysis

According to Section 2.2, information on the spatial availability and the calculation methods to determine the expected extractable heat must be provided.

As mentioned before, the decision which area may be eligible to install SGCs poses a sensible parameter in order to estimate the potential. We utilize the CLC dataset from 2018 [33] to identify suitable lands. The CLC dataset offers a comprehensive, European map that classifies any area into one of 44 classes. It is derived from satellite imagery and considers lands from a minimum mapping area of 25 ha. We preselect all classes from class 2, namely agricultural areas, since undeveloped land with little vegetation is generally suitable for excavation works and installation of SGCs. Due to minor development, paths, roads and other obstacles, we assume that 60 % of an area may be effectively occupied by SGCs.

Secondly, the standard **VDI 4640:2** for *Thermal use of the underground* through *Ground source heat pump systems* [28] by the Association of German Engineers is used to calculate the extractable heat. The calculation methods within the standard are based on Ramming [32]. The method accounts for typical consumption profiles of residential buildings, an alternating cycle of heat extraction and regeneration as well as heat pump temperature limits [28]. The calculation outputs the expected full load hours per year, area-specific heat flux and therefore a yearly quantity of heat. The heat from the SGC serves as evaporator heat for a downstream GSHP.

The method further requires input data on the soil type, for which we use a dataset on top soils in Germany provided by the Federal Institute for Geosciences and Natural Resources [34]. The dataset differentiates between 9 soil types, whereas as the **VDI 4640:2** demands for 4 main soil types. Therefore, a mapping was conducted utilizing the standard **DIN 4220** [35] and comparison to Carsel and Parrish [36], Bertermann et al. [37] and Ramming [32]. Secondly, the local climate conditions are taken into account according to the standard **DIN 4710** [38].

The standard provides calculation methods for multiple types of SGCs. We choose to estimate the potential for the standard horizontal ground heat collectors, consisting of polyethylene pipes of 32 mm × 3 mm.

Furthermore, assumptions concerning the Coefficient of Performance (*COP*) of potentially installed heat pumps need to be made. According to the AGFW [9], 71 % of DHNs in Germany are operated with water at temperatures of 90 °C or hotter. While typical values for *COPs* for (ground source) heat pumps that provide residential space heating and hot water often exceed 3 to 4, we attempt to determine a suitable *COP* value for integration into the current state of DHNs in Germany. Assuming a brine temperature of 10 °C and a Carnot efficiency of 0.5, we calculate a weighted *COP* of 2.6 to elevate the source temperature to an integrable flow temperature. For more details see Fig. C.11 in Appendix C. Lastly, we consider a heat loss of 11 % that occurs in-between source and consumer [9].

After determining the source of information on the geographical availability of shallow geothermal energy and defining the means of calculation for SGCs and therefore satisfying both conditions from Section 2.2, we need to select the spatial parameters in order to perform the algorithm from Fig. A.9. In order to find appropriate parameters, we define a set of possible values for $L_{\text{connection}}$ and L_{radius} as described in Section 2.2 to conduct a parameter study. We also vary the CLC classes that are considered eligible to install SGCs. We focus on a representative zone and evaluate the results to find parameters that are both realistic and show promising results. The examined cases are presented in Appendix C as well as some visualization of their results in Fig. C.12.

We select $L_{\text{connection}} = 500$ m, $L_{\text{radius}} = 1000$ m and CLC class *231*, which represents *Pastures, meadows and other permanent grasslands under agricultural use* [39]. These assumptions will be further discussed in Section 5.

For describing identified potentials, we differentiate between the actual, extracted SGE and the GSHP potential, taking the additional electric energy that supplies the heat pumps into consideration. The GSHPs operate with the previously calculated *COP* of 2.6. Furthermore, we define the coverage c_j by SGE or GSHP as the quotient of the potential $Q_{pot,j}$ by SGE or GSHP that was assigned to a DHN j and the grid's demand Q_j:

$$c_{j,\text{SGE/GSHP}} = \frac{Q_{\text{pot},j,\text{SGE/GSHP}}}{Q_j} \tag{4}$$

While the final heat demand Q_j can be fully satisfied by the GSHP's output if there are sufficient heat sources available, the coverage by SGE needs to account for the necessary exergetic elevation and therefore $c_{j,SGE}$ is numerically limited to $[0, 1 - \frac{1}{COP}]$. Referring to all DHNs found in Germany, we also define the total coverage c as the quotient of the total assigned potential Q_{pot} and the sum of all heat demands:

$$c_{\text{SGE/GSHP}} = \frac{Q_{\text{pot,SGE/GSHP}}}{\sum_j Q_j} \tag{5}$$

The evaluation shows a SGE potential of 15.31 TWh/a for the entirety of Germany. In due consideration of all assumptions, approximately 9.57 TWh/a of additional electric energy is needed to integrate the geothermal sources into the found heat grids, resulting in a GSHP potential of 24.87 TWh/a. Thus, the total coverage by SGE c_{SGE} amounts to 30.52 % and by GSHP c_{GSHP} to 49.59 %. Fig. 6 depicts the results by plotting the individual coverage c_j over the demand Q_j.

5. Discussion

This section discusses strengths and limitations of the methodology described in Section 2, as well as the deduced dataset presented in Section 3. Moreover, the dataset is differentiated from and compared to other available sources and datasets on DHNs. The proposed application in Section 4 is shortly discussed, as it does not pose the main feature of this study.

This study presents a methodology to identify and characterize DHNs for residential heat supply in Germany, resulting in the AixDHN dataset. It makes novel use of the recently published dataset of the census's survey on heating systems in residential buildings from 2022 [12] and therefore provides new insights into the current state of DHNs in Germany. The AixDHN dataset contains *estimated* information on the spatial location and shape within a 100 m-precision, the yearly heat demand, the amount and location of supplied apartments and heat density of 8,684 presumed DHNs. The methodology's overall strengths lie within the robust, generalized and systematic approach, which make it applicable throughout Germany without any further research on a regional level. These strengths are predominantly based on the comprehensive coverage of the census dataset and therefore rely on its accuracy. This dependence seems justified, since according to our extensive research, this source provides the most detailed, informative

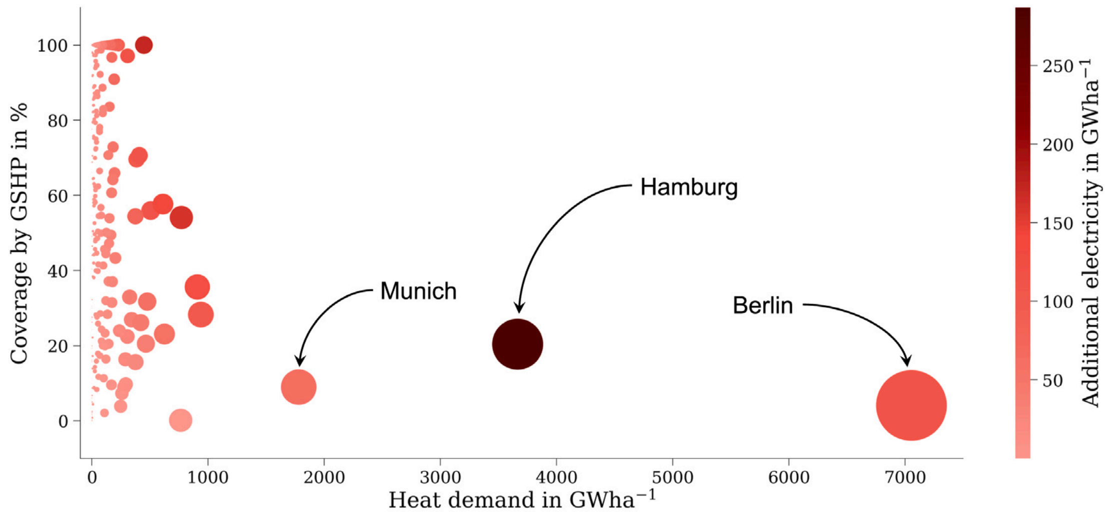

Fig. 6. Coverage by GSHP over demand for all found DHNs in Germany for a use case analysis of SGCs. The size and colour of the scatter point indicate the additional electricity required.

and recent dataset on DHNs in the context of spatial localization. However, some uncertainties are introduced, as the census must comply with conditions of anonymity and therefore an alteration of the data prior to publishment was performed [40]. In addition, the possibility of wrong statements by interviewees on their heating system cannot be ruled out. It is difficult to examine to which extent the original data was altered, but it appears plausible that especially in rural regions with small DHNs and few connected households, anonymization was necessary to protect personal data.

As briefly mentioned in Section 1, reliable information on the status quo of DHNs in Germany are currently restricted to few sources, such as selected energy atlases published by the states' responsible departments [8], the German Energy Efficiency Association for Heating, Cooling and CHP (AGFW) [9], the Halmstad University District Heating and Cooling database version 5 (HUDHC_v5) (which is not publicly available in its original form, but extracts are featured in [10]), the sEEnergies D5.1 District Heating dataset (sEE D5.1) [10] dataset (which is partly derived from HUDHC_v5) and few other sources such as ENERPIPE [13], Pelda et al. [11]. The range of information provided by the different sources varies significantly. On one hand, the AGFW provides yearly reports containing aggregated data with a nation-wide scope but little spatial context, while still being a frequently used source of information in this area of research. On the other hand, the state-dependent energy atlases [41–43] and datasets by companies such as ENERPIPE [13] provide more detailed descriptions of locations and technical details of some DHNs. Lastly, other scientific approaches by Fleiter et al. [10], Persson et al. [19], Möller et al. [44], Pelda et al. [11] attempt to combine systematic methodologies based on for example the heat demand density with individual research on operated networks. The majority of these sources have in common that they may contain more specific information regarding selected DHNs than the proposed AixDHN dataset, but lack the comprehensiveness that our methodology attempts to achieve. It must be recognized that some crucial technical characteristics such as flow temperatures, network lengths and heating capacity cannot be depicted in the AixDHN dataset. Specific research, surveys or other means of direct information gathering as conducted by the mentioned references seems inevitable to obtain these features.

As mentioned before, this study was able to identify 8,684 presumed DHNs. It can be observed that this figure is greater by a factor of at least two than the figure provided by the AGFW in their yearly report and by one magnitude than the data from HUDHC_v5. According to the AGFW and their evaluation of multiple unpublished statistical surveys, 4,188 DHNs were operated in Germany in 2022 [45]. This figure is not bound to residential DHNs and therefore cannot be directly compared to our figures, but it indicates a plausible order of magnitude. According to the HUDHC_v5, only 254 District Heating and Cooling (DHC) networks were operated within Germany in 2019 [10], although its incompleteness is commonly acknowledged [10] and the database seems to be limited to the larger systems in Germany.

While it is important to keep these discrepancies in mind and treat the results with caution, it is also necessary to acknowledge that our methodology was not developed nor is it suitable to determine the correct amount of DHNs in Germany. The choice of parameters used in the clustering process as explained in Section 2.1 affects the final figure of found DHNs significantly. Considering the distribution of area and demand of found DHNs as seen in Fig. 3(a) and Fig. 3(b), it seems plausible that many small DHNs in terms of area and demand were either falsely identified due to bad data or are in reality connected to a larger DHN nearby. Hence, the necessity of an adequate lower boundary as established in Section 2.1 is emphasized. On the contrary, it can be observed in Fig. 3(c) and Fig. B.10 that a very small number of DHNs, present in major German cities, represent large portions of the total residential district heating demand.

Section 2.2

We conclude that agreement on the absolute number of DHNs with other sources does not, by itself, improve the dataset's quality or usefulness for the intended use case in Section 2.2. Instead, the spatial characteristics of the identified presumed DH areas are more informative and should be prioritized. A pragmatic next step could be to derive a subset of the most significant DHNs to reduce the number of areas while preserving a high share of DH connection points according to the census. In this study, we retained the full set to provide a comprehensive baseline for future work, where such a selection would be reasonable.

Fig. 7(a) shows a comparison of the identified AixDHN networks (hatched, black areas) and the available information of the operating municipal utility company STAWAG (orange: currently operated area, yellow: area of further development) in the region and city of *Aachen* [46]. The depiction demonstrates the difficulties of choosing proper parameters to detect the narrow characteristics of real DHNs without compromising the broader connectivity between cluster points. The highlighted cutout furthermore confirms the constraint to residential DHN connection points, as the unidentified, upper part features exclusively commercial and public buildings.

Generally speaking, it can be seen that our DHN area overestimates the area of the currently operated grid, particularly in suburban regions

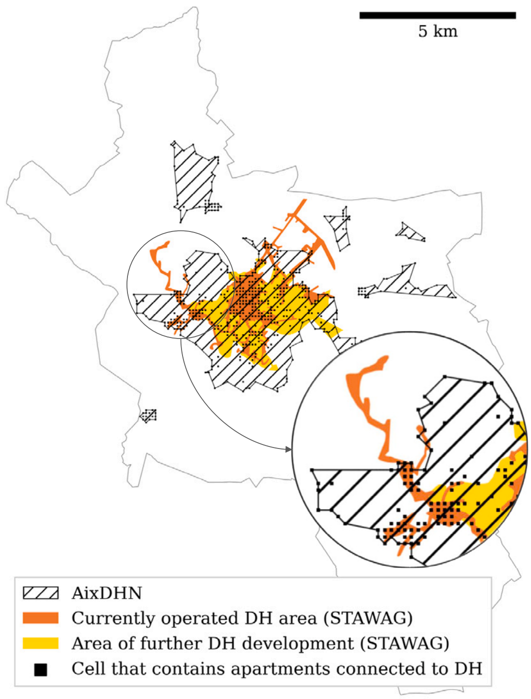

(a) Comparison with operated STAWAG network [46].

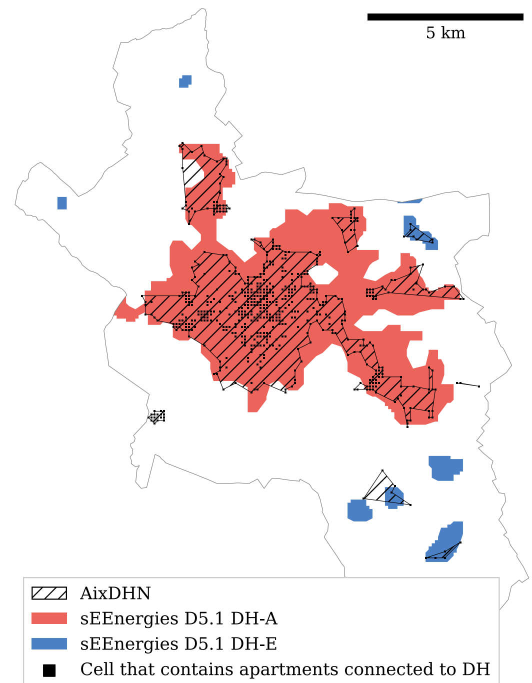

(b) Comparison with DH-E and DH-A from sEE D5.1 dataset [10].

Fig. 7. Comparison of the AixDHN dataset with external sources.

surrounding the city centre. According to our observations of multiple samples such as this one, we must assume a general overestimation of the identified area due to similar effects.

To further evaluate the quality of our dataset, we attempt to find a method of validation that can be employed on a larger scale and with full automation. As the review of other literature earlier in this section shows, there is no true source of validation data to compare our results to in terms of spatial characteristics. However, some work has been published on potentially feasible areas for DH systems. Fleiter et al. [10] presents the sEE D5.1 dataset by combining the HUDHC_v5 database [47,48] from 2019 and heat demand density data by hectare resolution based on the Pan-European Thermal Atlas (PETA 4.3) of the Heat Roadmap Europe 4 project [19,47] from 2018. The approach assumes general economic feasibility for DH in areas with yearly heat demand densities above $500\,\mathrm{GJ/(a\,ha)}$ and therefore defines Expected District Heating (DH-E) areas. Furthermore, information on the existence of DH within a city based on HUDHC_v5 is merged with found DH-E areas, resulting in Actual District Heating (DH-A) areas. The certainty about the spatial correctness of the dataset remains limited to the rather coarse indication on a municipal level by HUDHC_v5 and the general assumption of profitability for high heat demand areas. Fig. 7(b) illustrates the DH-E and DH-A datasets for the region of *Aachen* in comparison to our identified DHNs.

To compare our results to the sEE D5.1 dataset, we observe the occupied area and the amount of polygon areas listed in DH-E, DH-A as well as the union of both. Furthermore, we calculate the commonly used metric *Intersection over Union* (IoU), that represents the overlapping of two areas (see Eq. (6)), as well as the *Intersection over Area* (IoA) (see Eq. (7)), in which *Area* represents the area of our calculated results.

$$IoU = \frac{|\mathrm{comparison}| \cap |\mathrm{AixDHN}|}{|\mathrm{comparison}| \cup |\mathrm{AixDHN}|} \tag{6}$$

$$IoA = \frac{|A_{\mathrm{comparison}}| \cap |A_{\mathrm{AixDHN}}|}{|A_{\mathrm{AixDHN}}|} \tag{7}$$

The comparison is displayed in Table 2. It becomes obvious, that a majority of the areas within the AixDHN dataset can also be found in the sEE D5.1 dataset, resulting in a IoA value of 80.23 % for the union of DH-E and DH-A. However, with 41.29 %, only half of these matching areas are originating from the DH-A dataset. Since the DH-A dataset refers to mostly large cities and describes an area of $5{,}346.49\,\mathrm{km}^2$ with a relatively small amount of 221 polygons, it seems plausible that the condition of a high heat demand density results in extensive urban areas being classified as DH-A zones and therefore an overestimation of area. This effect can be observed in Fig. 7(b) surrounding the main DHN of *Aachen*. On the contrary, the DH-E dataset represents many small patches of land in rural regions that may be feasible for DH due to their local heat demand density. The intersection between our results and DH-E indicates that with $3{,}172.34\,\mathrm{km}^2$ a substantial portion of feasible but unconfirmed areas might already contain a DHN in operation. Some congruence in that regard can be seen in Fig. 7(b).

In general, the sEE D5.1 dataset covers twice the area of our dataset, which results in low overall IoU values. It also becomes clear that the spatially detailed census data is advantageous to characterize the shape of DHNs, especially in urban regions in which an identification merely based on the heat demand density is misleading. As stated before, we believe that our dataset overestimates the area of DHNs in suburban regions due to the clustering mechanism, but it does provide a major improvement in precision compared to the sEE D5.1 dataset.

The threshold for feasibility of DH of $500\,\mathrm{GJ/(a\,ha)}$ utilized by Fleiter et al. [10] and Persson et al. [19] translates to $13.89\,\mathrm{GWh/(a\,km^2)}$ and is going to be utilized as a preliminary benchmark. Fig. 4(b) demonstrates that the overall residential heat demand density within the AixDHNs regions (red line, attribute **heat_density**) is predominantly above this threshold. This indicates that most identified DHNs feature an adequately high heat demand density in theory. However, regarding the demand that has been actually attributed towards DH (blue line, attribute **heat_density_DH**), the identified density remains below the

Table 2
Comparison of the AixDHN dataset with the DH-E/DH-A datasets of the sEE D5.1 dataset.

	AixDHN	DH-E	DH-A	DH-E ∪ DH-A
Area in km^2	8,146.13	11,028.18	5,346.49	16,374.67
Polygon count	8,684	13,232	221	13,453
		Comparison with AixDHN		
Intersection in km^2		3,172.34	3,363.40	6,535.74
IoU in %		19.82	33.20	36.34
IoA in %		38.94	41.29	80.23

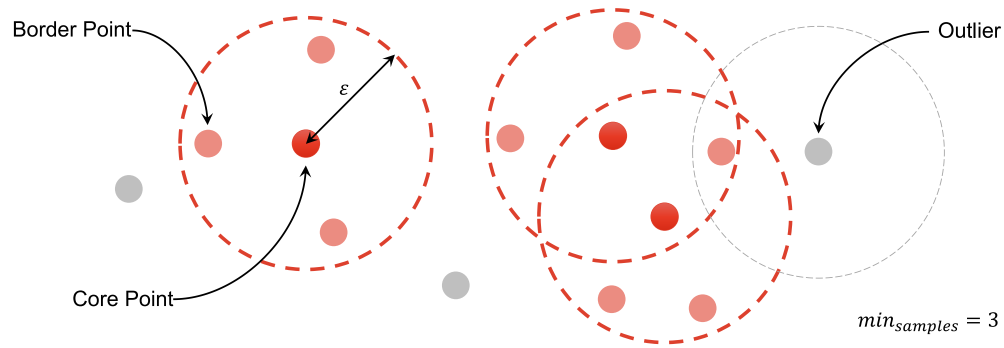

Fig. A.8. Schematic application of DBSCAN on an exemplary point cloud.

threshold, supporting the impression of overestimation of area. Nevertheless, the former can be understood as an indication on further potential for DH within that area. Additionally, Fleiter et al. [10] takes non-residential demands into account, while this study intentionally utilizes the hotmaps dataset on residential demands only [16]. In terms of the hotmaps dataset itself, it shall be mentioned that it was published in 2016 and determines the energy demand based on regional indicators using a statistical approach [22,49]. This renders it suitable for strategic estimations and high-level energy planning, however, it does not account for local specificities [49] . Therefore, it must be viewed critically when applied to spatially detailed or site-specific planning contexts.

Focusing on the proposed application of the derived AixDHN dataset – namely, estimating the potential of renewable energy sources located in the vicinity of identified DHNs – several general limitations must be acknowledged. First and foremost, no information on the hydraulic structure of the identified DHNs is available. Consequently, the approach employed in this study, which relies solely on the spatial distance between a heat source and the outer boundary of a DHN, does not allow for the identification of technically feasible points of heat integration. Moreover, compatibility aspects between a given heat source and the existing DHN, such as temperature levels or temporal availability of heat, cannot be assessed due to the lack of corresponding data within the AixDHN dataset. The primary aim of the analysis is to assess the general spatial accessibility of renewable heat sources rather than to identify exact integration points.

The use case presented in Section 4, which explores the integration of SGCs into the identified DHNs, is briefly addressed here. The potential estimation is conducted from a purely technical perspective, without incorporating any economic evaluation. The estimation of available potential is based on simplified guidelines provided by the Association of German Engineers [28], which are generally suited to the scope of this assessment. Originally intended for smaller-scale SGC applications, these guidelines were adapted and extended to fit the context of this study. As such, the resulting potential analysis does not comprehensively cover all technically or contextually relevant factors, but rather offers an indicative estimation of the potential's overall magnitude. The earlier addressed problem of uncertainty of network temperatures and thus uncertainty of realistic *COPs* for integrating SGE into found DHNs is solved here by estimating a weighted average *COP* as described in Section 4 and Fig. C.11. In order to select the parameters relevant for calculating the DHN's individual potential according to Section 2.2, a parameter study is conducted. In terms of the preselection of eligible areas for installation of SGCs, this study utilizes the CLC dataset and examines the classes of agricultural use, which appear to be the most realistic according to applied examples [50–52] and similar potential analyses [53]. For the final potential analysis, only the CLC class 231, that includes pastures, meadows and other grasslands is considered, since these areas show little cultivation and most likely little to no conflict of usage is present. Lastly, the assumption of a usability of 60 % is based on a rough estimation after investigating the accuracy of the CLC dataset through comparison with current satellite imagery. Apart from this, further relevant parameters are the maximum distance surrounding the DHN L_{radius}, within which a SGC system can be installed, and the maximum distance for the connection pipeline to the DHN $L_{\text{connection}}$. Since the economic feasibility of heat transport over long distances strongly depends on aspects such as the installed capacity, expectable full-load hours [53] and features of the traversed land [54], the choice of spatial parameters is challenging. An analysis of the Federal Environment Agency [53] utilizes a 1,000 m radius for solar thermal systems, and Fleiter et al. [10] a 10 km radius for industrial excess heat recovery. Given the rather small temperature difference of 3 K to 4 K of SGE, we investigated a range of distances as described in Section 4 and summarized in Table C.3. Fig. C.12 shows that the determined potential is sensible to both spatial parameters, especially at low values. The choice of $L_{\text{connection}} = 500$ m and $L_{\text{radius}} = 1{,}000$ m poses an advantageous compromise, as the potential barely increases with higher spatial thresholds.

6. Conclusion

In conclusion, this work demonstrates a systematic modelling approach to identify and characterize 8,684 residential DHNs across Germany using 2022 census data and clustering algorithms. This represents a significant advancement over existing data sources, which are either limited in scope (HUDHC [48]: 254 networks) or lack spatial detail (AGFW [9]: 4188 networks).

Validation against the sEE D5.1 dataset of economically viable areas for DH supply showed strong agreement, with an Intersection over Area (IoA) of 80.23 %, confirming the robustness of the proposed

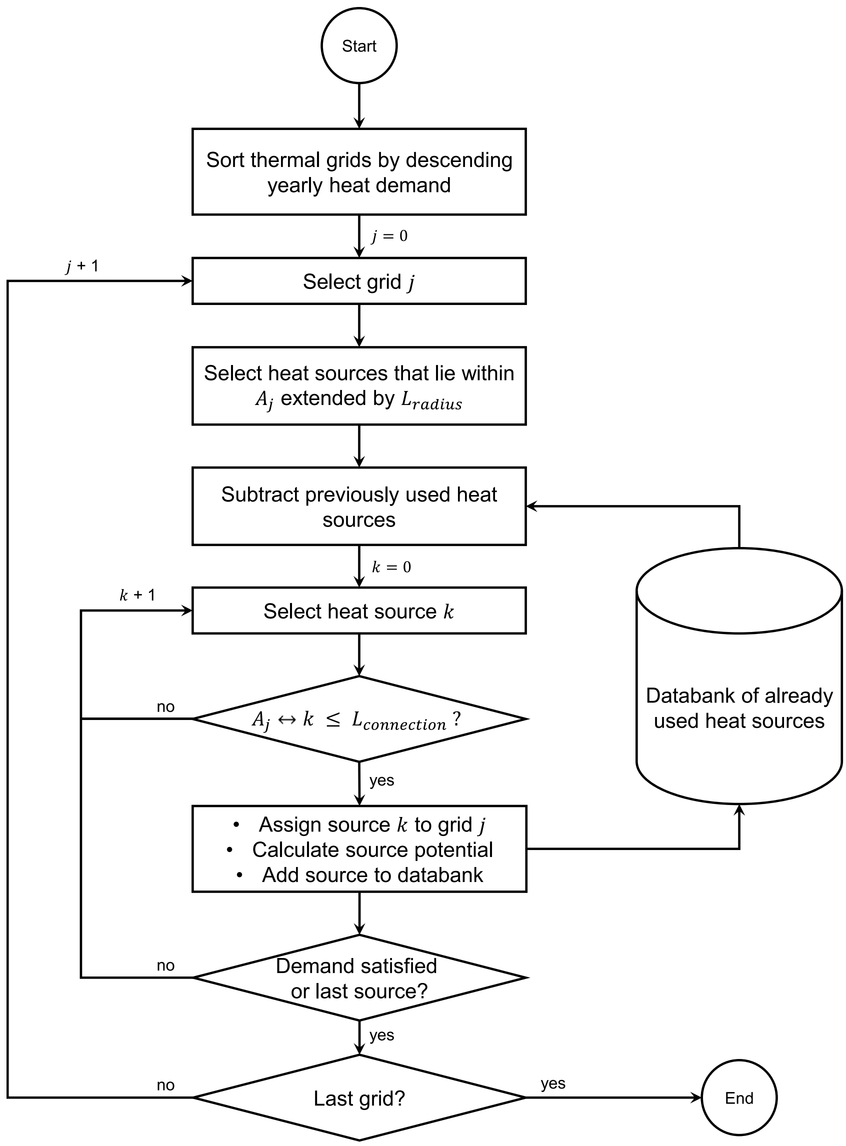

Fig. A.9. Algorithm for assigning renewable heat sources to surrounding DHNs by spatial parameters $L_{connection}$ and L_{radius}. $A_j \leftrightarrow k$ describes the shortest distance between a source k and the area of a DHN j.

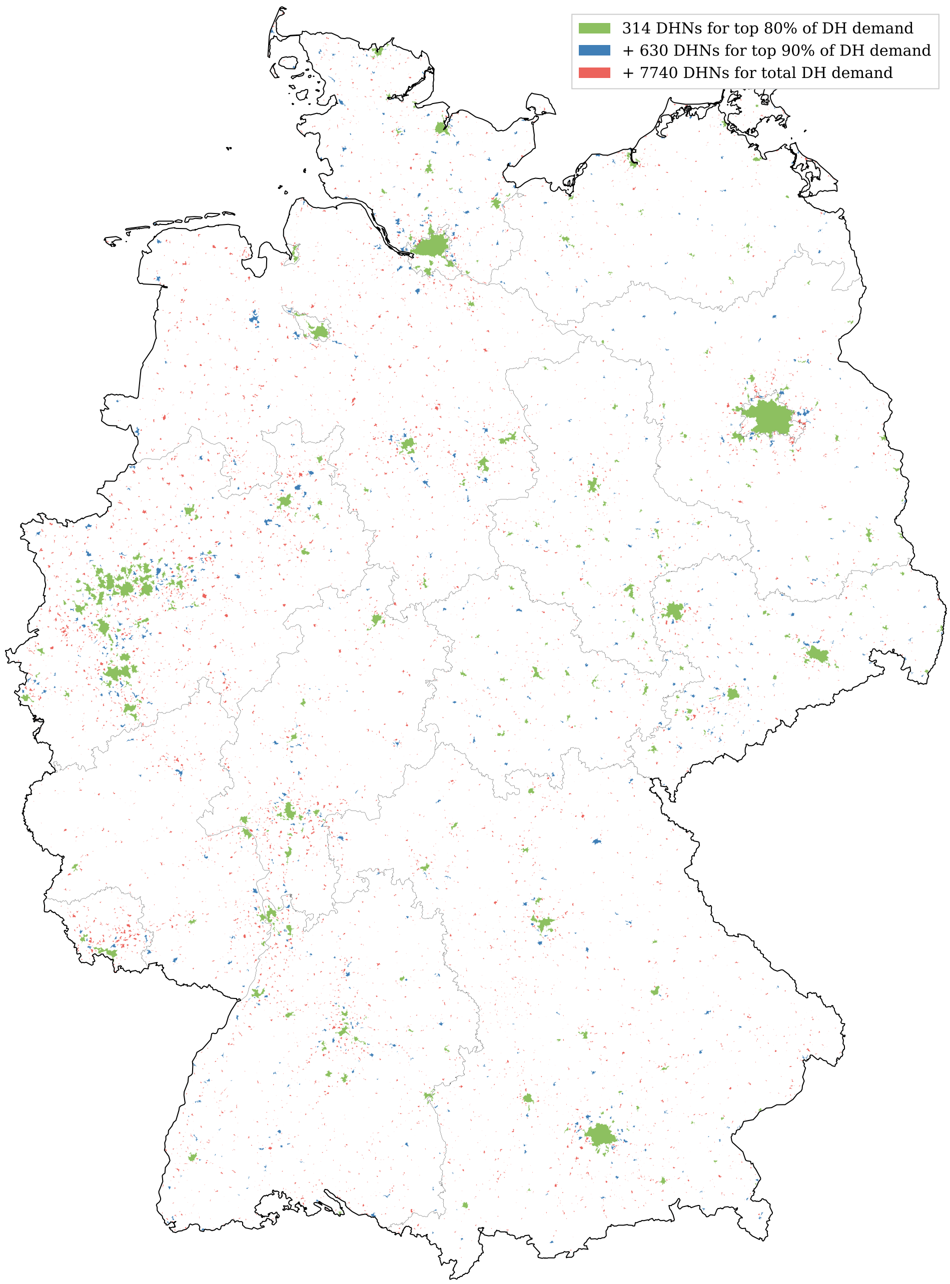

Fig. B.10. Spatial overview of all identified DHNs in Germany. The 314 green coloured networks suffice 80 % of the total DH demand, the 630 blue coloured networks further increase the representation to 90 % and the 7,740 red coloured networks describe the final 10 %.

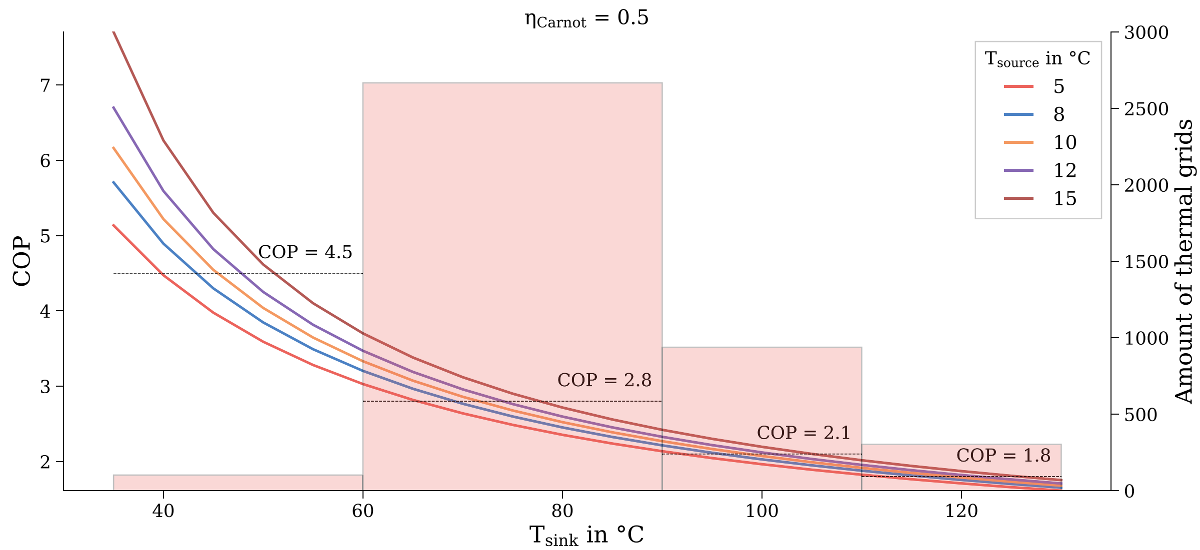

Fig. C.11. Estimation of *COP* for integration of SGE into DHNs. Left axis: *COP* for a range of source temperatures as a function of network temperature and with a Carnot efficiency of 50 %. Right axis: amount of DHNs within that temperature interval according to [9].

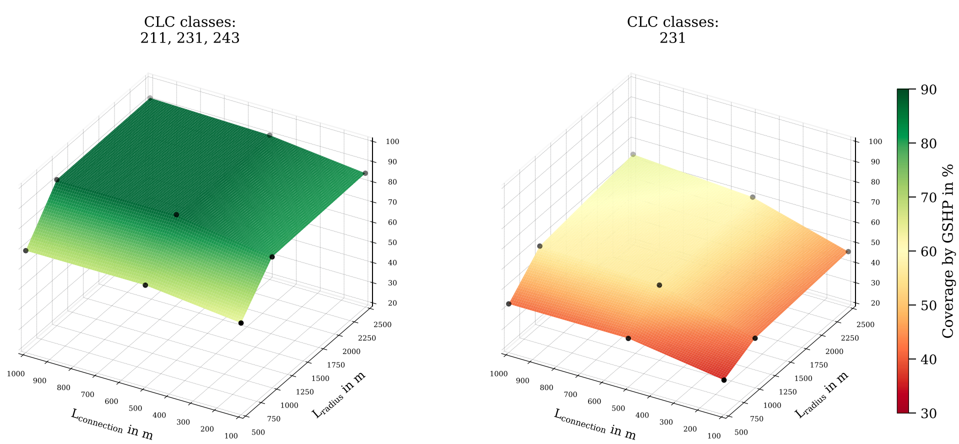

Fig. C.12. Extract from results of parameter study for SGC use case. Potential for representative zone of *Hessen*. Coverage by GSHP defined according to Eq. (5) with respect to a *COP* of 2.6.

methodology despite moderate overestimations in suburban zones. The dataset enables high-resolution assessment of renewable heat source integration potential, as demonstrated through the exemplary SGC use case which revealed significant deployment opportunities.

Future research could enhance the clustering algorithm to follow street layouts and integrate actual DHN infrastructure plans for improved calibration. The methodology could also be extended to other renewable technologies, such as Shallow Geothermal Probes (SGPs), once adequate subsurface data like Wärmegut [55] becomes nationwide available.

This methodology provides a robust baseline dataset for Germany's heating sector transformation and renewable energy integration planning.

Glossary

COP Coefficient of Performance

AGFW German Energy Efficiency Association for Heating, Cooling and CHP

AixDHN District Heating Networks Dataset from Clustered Census Data

CLC Corine Land Cover

DBSCAN Density-Based Spatial Clustering of Applications with Noise

DH District Heating

DH-A Actual District Heating

DH-E Expected District Heating

DHC District Heating and Cooling

DHN District Heating Network

GSHP Ground Source Heat Pump

HUDHC_v5 Halmstad University District Heating and Cooling database version 5

sEE D5.1 sEEnergies D5.1 District Heating dataset

SGC Shallow Geothermal Collector

SGE Shallow Geothermal Energy

SGP Shallow Geothermal Probe

WKT Well Known Text

Table C.3
Parameter values of selected CLC classes and corresponding $L_{connection}$ and L_{radius} used in the SGC case study.

CLC classes (according to [56])	$L_{connection}$ [m]	L_{radius} [m]
211, 221, 222, 231, 242, 243	1000	2500
211, 231, 243	500	1000
231, 243	100	500
231		
211, 231		

CRediT authorship contribution statement

Kai Droste: Writing – review & editing, Writing – original draft, Visualization, Validation, Resources, Project administration, Methodology, Investigation, Formal analysis, Data curation, Conceptualization. **Luca Döring:** Writing – original draft, Visualization, Validation, Software, Resources, Methodology, Formal analysis, Data curation. **Jonas Klingebiel:** Writing – review & editing, Supervision, Project administration. **Rahul Karuvingal:** Writing – review & editing, Formal analysis. **Dirk Müller:** Writing – review & editing, Supervision, Funding acquisition.

Declaration of competing interest

The authors declare that they have no known competing financial interests or personal relationships that could have appeared to influence the work reported in this paper.

Acknowledgements

This research was funded by the Federal Ministry for Economic Affairs and Energy (BMWE) and EU grant numbers 03EWR020E.

Appendix A. Methodology

See Figs. A.8 and A.9.

Appendix B. Results

See Fig. B.10.

Appendix C. Use case

See Figs. C.11 and C.12.
See Table C.3.

Data availability

The Data is available on github: https://github.com/RWTH-EBC/AixDHN.

References

[1] European Climate Law - European Commission. URL: https://climate.ec.europa.eu/eu-action/european-climate-law_en.
[2] Climate Change Act: Climate neutrality by 2045. url: . 2021,.
[3] Agentur für Erneuerbare Energien. Endenergieverbrauch nach Strom, Wärme und Verkehr. 2024, URL: https://www.unendlich-viel-energie.de/mediathek/grafiken/energieverbrauch-in-deutschland-im-jahr-2023-nach-strom-waerme-und-verkehr.
[4] BEDW. Wie heizt Deutschland? - Ergebnisbericht. 2024, URL: https://www.bdew.de/media/documents/Wie_heizt_Deutschland_2023_-aktualisierte_Fassung-_BDEW_1.pdf.
[5] Agentur für Erneuerbare Energien. Fernwärmeerzeugung nach Energieträgern in Deutschland 2023. 2023, URL: https://www.unendlich-viel-energie.de/mediathek/grafiken/fernwaermeerzeugung-nach-energietraegern-in-deutschland-2023.
[6] Kommunale wärmeplanung. 2025, URL: https://www.bmwsb.bund.de/SharedDocs/faqs/Webs/BMWSB/DE/kwp/kwp-liste.html?nn=21194376.
[7] Gesetz für die Wärmeplanung und zur Dekarbonisierung der Wärmenetze (Wärmeplanungsgesetz - WPG). 2024.
[8] KWW Kommunale Wärmewende. 2024, URL: https://www.kww-halle.de/wissen.
[9] AGFW - Der Energieeffizienzverband für Wärme, Kälte und KWK eV. AGFW Hauptbericht 2023. Technical Report, AGFW - Der Energieeffizienzverband für Wärme, Kälte und KWK e.V.; 2024, Read_Status: New Read_Status_Date: 2025-01-27T13:38:58.035Z.
[10] Fleiter T, Manz P, Neuwirth M, Mildner F, Persson U, Kermeli K, Crijns-Graus W, Rutten C. Documentation on excess heat potentials of industrial sites including open data file with selected potentials. 2020, http://dx.doi.org/10.5281/ZENODO.4785411, URL: https://zenodo.org/record/4785411.
[11] Pelda J, Holler S, Persson U. District heating atlas - Analysis of the German district heating sector. Energy 2021;233:121018. http://dx.doi.org/10.1016/j.energy.2021.121018, URL: https://linkinghub.elsevier.com/retrieve/pii/S0360544221012664.
[12] Bundesamt S. Zensus 2022 - Ergebnisse. 2024, URL: https://www.zensus2022.de/DE/Ergebnisse-des-Zensus/_inhalt.html.
[13] ENERPIPE. ENERPIPE Wärmenetze in Deutschland. 2025, URL: https://www.enerpipe.de/projekte/uebersicht-karte.
[14] Wirtz M, Schreiber T, Müller D. Survey of 53 Fifth-Generation District Heating and Cooling (5GDHC) Networks in Germany. Energy Technol 2022;10(11):2200749. http://dx.doi.org/10.1002/ente.202200749, URL: https://onlinelibrary.wiley.com/doi/10.1002/ente.202200749.
[15] Bundesamt S. Zensus 2022 - Gebäude- und Wohnungszählung. 2024, URL: https://www.zensus2022.de/DE/Wer-wurde-befragt/Gebaeude_und_Wohnungszaehlung.html?nn=352818#.
[16] Team H. Hotmaps - The open source mapping and planning tool for heating and cooling. 2016, URL: https://www.hotmaps.eu/map.
[17] Landesämter S. EVAS 43411 - Jahreserhebung über Erzeugung und Verwendung von Wärme sowie über den Betrieb von Wärmenetzen. 2022, Read_Status: New Read_Status_Date: 2025-03-24T06:36:35.256Z.
[18] Bundesamt S. Zensus 2022 - Atlas. 2024, URL: https://atlas.zensus2022.de/.
[19] Persson U, Wiechers E, Möller B, Werner S. Heat Roadmap Europe: Heat distribution costs. Energy 2019;176:604–22. http://dx.doi.org/10.1016/j.energy.2019.03.189, URL: https://linkinghub.elsevier.com/retrieve/pii/S0360544219306097.
[20] Ester M, Kriegel H-P, Sander J, Xu X. A Density-Based Algorithm for Discovering Clusters in Large Spatial Databases with Noise. In: Proceedings of the second international conference on knowledge discovery and data mining. KDD '96, AAAI Press; 1996, p. 226–31.
[21] Concave Hull Python Package. 2023, URL: https://concave-hull.readthedocs.io/en/latest/.
[22] Pezzutto S, Kranzl L, Zambotti S, Croce S, Zambelli P, Scaramuzzino C, Pascuas RP, Haas F, Lucchi E, Valle ND, Zubaryeva A, Müller A. Hotmaps D2.3 WP2 Report – Open Data Set for the EU28. Technical Report, 2019.
[23] Umweltbundesamt, Arbeitsgemeinschaft Energiebilanzen. Anteile der Anwendungsbereiche am Endenergieverbrauch der privaten Haushalte 2008 und 2022. 2023, URL: https://www.umweltbundesamt.de/daten/private-haushalte-konsum/wohnen/energieverbrauch-privater-haushalte#hochster-anteil-am-energieverbrauch-zum-heizen.
[24] Loga T, Stein B, Diefenbach N, Born R. Deutsche Wohngebäudetypologie: beispielhafte Maßnahmen zur Verbesserung der Energieeffizienz von typischen Wohngebäuden, 2., erw. Aufl. Darmstadt: IWU; 2015,
[25] Döring L, Droste K. EBC - District Heating Networks Dataset from Clustered Census Data. 2025, URL: https://github.com/RWTH-EBC/AixDHN.
[26] Bundesamt für Kartographie und Geodäsie. Verwaltungsgebiete 1:250 000 Stand 01.01. (VG250 01.01.) ©GeoBasis-DE / BKG (2024). 2024, URL: https://www.bkg.bund.de.
[27] Gillies S. The Shapely User Manual. 2025, URL: https://shapely.readthedocs.io/en/2.0.7/manual.html#id22.
[28] VDI Verein Deutscher Ingenieure. VDI 4640 Blatt 2:2019-06 Thermische Nutzung des Untergrunds - Erdgekoppelte Wärmepumpenanlagen. 2019.
[29] Stober I, Bucher K. Geothermie. Berlin, Heidelberg: Springer Berlin Heidelberg; 2020, http://dx.doi.org/10.1007/978-3-662-60940-8, URL: http://link.springer.com/10.1007/978-3-662-60940-8.
[30] Moeck I, Weber J. Metastudie zur nationalen Erdwärmestrategie. Technical Report, Leibniz-Institut für Angewandte Geophysik; 2022.
[31] VDI Verein Deutscher Ingenieure. VDI 4640 Blatt 1:2021-12 Thermische Nutzung des Untergrunds - Grundlagen, Genehmigungen, Umweltaspekte. 2021.
[32] Ramming K. Bewertung und optimierung oberflächennaher erdwärmekollektoren für verschiedene lastfälle (Ph.D. thesis), TU Dresden; 2007.
[33] Copernicus. CORINE Land Cover übersicht. 2018, URL: https://land.copernicus.eu/en/products/corine-land-cover.
[34] Bundesanstalt für Geowissenschaften und Rohstoffe. Bodenarten der Oberböden Deutschlands 1:1.000.000. 2007, URL: https://www.bgr.bund.de/DE/Themen/Boden/Informationsgrundlagen/Bodenkundliche_Karten_Datenbanken/Themenkarten/BOART1000OB/boart1000ob_node.html.

[35] DIN Deutsches Institut für Normung eV. DIN 4220:2020-11, Bodenkundliche Standortbeurteilung_- Kennzeichnung, Klassifizierung und Ableitung von Bodenkennwerten (normative und nominale Skalierungen). 2020, http://dx.doi.org/10.31030/3181018, URL: https://www.dinmedia.de/de/-/-/326179931.

[36] Carsel RF, Parrish RS. Developing joint probability distributions of soil water retention characteristics. Water Resour Res 1988;24(5):755–69. http://dx.doi.org/10.1029/WR024i005p00755, URL: https://agupubs.onlinelibrary.wiley.com/doi/10.1029/WR024i005p00755.

[37] Bertermann D, Schwartz H, Wagner J, Rammler M. Erarbeitung eines Handlungsleitfadens zur Abschätzung der oberflächennahen geothermischen Potentiale in ländlichen Gemeinden. In: FAUErlangen-Nürnberg, editor. Technical Report F/G4-/503, 2019, URL: https://www.arc.ed.tum.de/fileadmin/w00cgv/klima/Publikationen/Berichte/Leitfaden_Energienutzungsplan.pdf.

[38] DIN Deutsches Institut für Normung eV. DIN 4710:2003-01, Statistiken meteorologischer Daten zur Berechnung des Energiebedarfs von heiz- und raumlufttechnischen Anlagen in Deutschland. 2003, http://dx.doi.org/10.31030/9258155, URL: https://www.dinmedia.de/de/-/-/49623776.

[39] Copernicus. CORINE Land Cover 2018 (vector/raster 100 m), Europe, 6-yearly. 2018, URL: https://land.copernicus.eu/en/products/corine-land-cover/clc2018.

[40] Statistische Ämter des Bundes und der Länder. Geheimhaltung mit Cell-Key-Methode. 2024, URL: https://www.statistikportal.de/de/cell-key-methode.

[41] Bayerisches Staatsministerium für Wirtschaft, Landesentwicklung und Energie. Energieatlas Bayern. 2025, URL: https://www.energieatlas.bayern.de/thema_energie/waermenetze.

[42] LUBW Landesanstalt für Umwelt Baden-Württemberg. Energieatlas Baden-Württemberg. 2025, URL: https://www.energieatlas-bw.de/.

[43] Senatsverwaltung für Wirtschaft, Energie und Betriebe Berlin. Energieatlas Berlin. 2025, URL: https://energieatlas.berlin.de/.

[44] Möller B, Wiechers E, Persson U, Grundahl L, Lund RS, Mathiesen BV. Heat Roadmap Europe: Towards EU-Wide, local heat supply strategies. Energy 2019;177:554–64. http://dx.doi.org/10.1016/j.energy.2019.04.098, URL: https://linkinghub.elsevier.com/retrieve/pii/S0360544219307315.

[45] AG Energiebilanzen eV, Fraunhofer ISI, RWI -Leibniz-Institut für Wirtschaftsforschung, TU München. Anwendungsbilanzen zur Energiebilanz Deutschland - Endenergieverbrauch nach Energieträgern und Anwendungszwecken. Technical Report, AG Energiebilanzen e.V.; 2023, URL: https://ag-energiebilanzen.de/daten-und-fakten/auswertungstabellen/.

[46] STAWAG Aachen. Fernwärmeplan STAWAG Aachen. 2022, URL: https://www.stawag.de/produkte/waerme/#c4303.

[47] Persson U, Möller B, Wiechers E. Methodologies and Assumptions Used in the Mapping: deliverable 2.3: A Final Report Outlining the Methodology and Assumptions Used in the Mapping. Technical Report, Heat Roadmap Europe; 2017.

[48] Persson U, Möller B, Werner S. Heat Roadmap Europe: Identifying strategic heat synergy regions. Energy Policy 2014;74:663–81. http://dx.doi.org/10.1016/j.enpol.2014.07.015, URL: https://linkinghub.elsevier.com/retrieve/pii/S0301421514004194.

[49] Müller A, Hummel M, Kranzl L, Fallahnejad M, Büchele R. Open Source Data for Gross Floor Area and Heat Demand Density on the Hectare Level for EU 28. Energies 2019;12(24):4789. http://dx.doi.org/10.3390/en12244789, URL: https://www.mdpi.com/1996-1073/12/24/4789.

[50] Zeh R, Ohlsen B, Philipp D, Bertermann D, Kotz T, Jocić N, Stockinger V. Large-Scale Geothermal Collector Systems for 5th Generation District Heating and Cooling Networks. Sustainability 2021;13(11):6035. http://dx.doi.org/10.3390/su13116035, URL: https://www.mdpi.com/2071-1050/13/11/6035.

[51] Brennenstuhl M, Zeh R, Otto R, Pesch R, Stockinger V, Pietruschka D. Report on a Plus-Energy District with Low-Temperature DHC Network, Novel Agrothermal Heat Source, and Applied Demand Response. Appl Sci 2019;9(23):5059. http://dx.doi.org/10.3390/app9235059, URL: https://www.mdpi.com/2076-3417/9/23/5059.

[52] Zeh R, Stockinger V, Ohlsen B. Kalte Nahwärmenetze und oberflächennaheste Geothermie im urbanen Raum. 2019.

[53] Ortner S, Pehnt M, Blömer S, Auberger A, Jan Steinbach, Deurer J, Popovski E, Lösch O, Langreder N, Thamling N, Sahnoun M, Rau D. Analyse des wirtschaftlichen Potenzials für eine effiziente Wärme- und Kälteversorgung: Beitrag zur Berichtspflicht EnEff-RL, Artikel 14 - Anhang VIII. In: Umweltbundesamt, editor. 2021.

[54] Sandrock M, Maaß C, Weisleder S, Westholm H, Schulz W, Kreuter H, Baisch C, Löschan G, Reyer D, Mangold D, Riegger M, Köhler C. Kommunaler Klimaschutz durch Verbesserung der Effizienz in der Fernwärmeversorgung mittels Nutzung von Niedertemperaturwärmequellen am Beispiel tiefengeothermischer Ressourcen. In: Umweltbundesamt, editor. Umweltbundesamt; 2018.

[55] Landesamt für Umwelt- und Arbeitsschutz (LUA) des Saarlandes. WärmeGut-03EE4046I. 2025, URL: https://www.enargus.de/detail/?id=132064266.

[56] Kosztra B, Büttner G. Updated CLC Illustrated Nomenclature Guidelines. Technical Report, European Environment Agency; 2019, Read_Status: New Read_Status_Date: 2024-10-09T13:40:43.802Z.